

Constraints on modified gravity from the observed X-ray luminosity function of galaxy clusters

David Rapetti^{1*}, Steven W. Allen¹, Adam Mantz¹ and Harald Ebeling²

¹ *Kavli Institute for Particle Astrophysics and Cosmology at*

Stanford University, 452 Lomita Mall, Stanford 94305-4085, CA, USA, and

SLAC National Accelerator Laboratory, 2575 Sand Hill Road, Menlo Park 94025, CA, USA.

² *Institute for Astronomy, 2680 Woodlawn Drive, Honolulu, HI 96822, USA*

Accepted ???, Received ???; in original form 25 October 2018

ABSTRACT

We use measurements of the growth of cosmic structure, as inferred from the observed evolution of the X-ray luminosity function (XLF) of galaxy clusters, to constrain departures from General Relativity (GR) on cosmological scales. We employ the popular growth rate parameterization, $\Omega_m(z)^\gamma$, for which GR predicts a growth index $\gamma \sim 0.55$. We use observations of the cosmic microwave background (CMB), type Ia supernovae (SNIa), and X-ray cluster gas-mass fractions (f_{gas}), to simultaneously constrain the expansion history and energy content of the Universe, as described by the background model parameters: Ω_m , w , and Ω_k , i.e., the mean matter density, the dark energy equation of state parameter, and the mean curvature, respectively. Using conservative allowances for systematic uncertainties, in particular for the evolution of the mass–luminosity scaling relation in the XLF analysis, we find $\gamma = 0.51_{-0.15}^{+0.16}$ and $\Omega_m = 0.27 \pm 0.02$ (68.3 per cent confidence limits), for a flat cosmological constant (Λ CDM) background model. Allowing w to be a free parameter, we find $\gamma = 0.44_{-0.15}^{+0.17}$. Relaxing the flatness prior in the Λ CDM model, we obtain $\gamma = 0.51_{-0.16}^{+0.19}$. When in addition to the XLF data we use the CMB data to constrain γ through the ISW effect, we obtain a combined constraint of $\gamma = 0.45_{-0.12}^{+0.14}$ for the flat Λ CDM model. Our analysis provides the tightest constraints to date on the growth index. We find no evidence for departures from General Relativity on cosmological scales.

Key words: cosmological parameters – cosmology: observations – cosmology: theory – X-ray: galaxies: clusters

1 INTRODUCTION

Recently, using the observed evolution of the X-ray luminosity function (XLF) of massive galaxy clusters, Mantz et al. (2008, hereafter M08) presented new constraints on dark energy from measurements of the growth of cosmic structure (see also Vikhlinin et al. 2009). These results are consistent with and complementary to those based on measurements of the cosmic expansion history, as deduced from distances to type Ia supernovae (Riess et al. 1998; Perlmutter et al. 1999; Davis et al. 2007; Kowalski et al. 2008), the gas mass fraction in galaxy clusters (Allen et al. 2004, 2008; Rapetti et al. 2005, 2007), and Baryon Acoustic Oscillations in the distribution of galaxies (Cole et al. 2005; Eisenstein et al. 2005; Percival et al. 2007). In combination with independent measurements of the cosmic microwave background (Spergel et al. 2003; Spergel et al.

2007; Komatsu et al. 2009), such measurements argue for a universe that is spatially flat, with most matter being cold and dark, and with the energy density being currently dominated by a cosmological constant, Λ .

Due to severe theoretical problems associated with the cosmological constant, a plethora of other dark energy models have been proposed (for a review, see Frieman et al. 2008). Recent works (Carroll et al. 2006; Caldwell et al. 2007; Hu & Sawicki 2007; Amin et al. 2008; Bertschinger & Zukin 2008, and references therein) have studied the possibility that late-time cosmic acceleration is not driven by dark energy but rather by gravity. These authors propose various frameworks to test for both time and scale-dependent modifications to GR at late times and on large scales. Although, currently, modifications to GR may be argued to be theoretically disfavoured, it is essential to test for such deviations using powerful, new data that are now becoming available. To measure departures from GR on cosmological scales, experiments sensitive to the dy-

* Email: drapetti@slac.stanford.edu

namical effects of GR on these scales are required. Such experiments include, for example, the cross-correlation of the integrated Sachs-Wolfe (ISW) effect with other matter tracers; galaxy clustering; weak gravitational lensing; or cluster number counts using, e.g., X-ray selected samples.

General Relativity has been thoroughly tested from laboratory to Solar System scales. However, GR has only just begun to be tested on cosmological scales. Several authors have recently investigated a simple parameterization of the growth rate, $\Omega_m(z)^\gamma$ (first introduced by Peebles 1980), to test for time-dependent modifications to GR (see e.g. Linder 2005; Sapone & Amendola 2007; Polarski & Gannouji 2008; Gannouji & Polarski 2008; Acquaviva et al. 2008; Ballesteros & Riotta 2008; Mortonson et al. 2009; Thomas et al. 2009). For a growth index, γ , of approximately 0.55, this parameterization accurately models the growth rate of GR. Some authors (Nesseris & Perivolaropoulos 2008; Di Porto & Amendola 2008; Wei 2008; Gong 2008) have recently estimated constraints on γ by combining results from measurements of redshift space distortions and evolution in the galaxy power spectrum, as well as measurements of the normalization of the matter power spectrum, $\sigma_8(z)$, from Lyman- α forest data. Using current cosmic shear and galaxy clustering data at low redshift, Dore et al. (2007) placed constraints on scale-dependent modifications to GR. These authors constrained two phenomenological, although physically motivated, modifications of the Poisson equation on megaparsec scales (from 0.04 to 10 Mpc).

In this paper, we use the XLF experiment developed by M08, and data from the *ROSAT* Brightest Cluster Sample (BCS; Ebeling et al. 1998), the *ROSAT*-ESO Flux Limited X-ray cluster sample (REFLEX; Böhringer et al. 2004), the MASSive Cluster Survey (MACS; Ebeling et al. 2001) and the 400 square degrees *ROSAT* PSPC cluster survey (400sd; Burenin et al. 2007), to constrain departures from GR on scales of tens of megaparsecs over the redshift range $z < 0.9$. We use CMB (Komatsu et al. 2009), SNIa (Kowalski et al. 2008), and cluster f_{gas} data (Allen et al. 2008) to simultaneously constrain the background evolution of the Universe. We examine three background models: flat Λ CDM, flat w CDM and non-flat Λ CDM. We employ a Markov Chain Monte Carlo (MCMC) analysis, accounting for systematic uncertainties in the experiments. Our results represent the first constraints on γ from the observed growth of cosmic structure in galaxy clusters.

2 PARAMETERIZING THE GROWTH OF COSMIC STRUCTURE

In GR, the evolution of the linear matter density contrast $\delta \equiv \delta\rho_m/\rho_m$, where ρ_m is the mean comoving matter density and $\delta\rho_m$ a matter density fluctuation, can be calculated in the synchronous gauge by solving the scale-independent equation

$$\ddot{\delta} + 2\frac{\dot{a}}{a}\dot{\delta} = 4G\pi\rho_m\delta, \quad (1)$$

where ‘dot’ represents a derivative with respect to time, and a is the cosmic scale factor.

Following Lahav et al. (1991) and Wang & Steinhardt (1998), several authors (see e.g. Huterer & Linder 2007;

Linder & Cahn 2007) have parameterized the evolution of the growth rate as $f(a) \equiv d \ln \delta / d \ln a = \Omega_m(a)^\gamma$. Recasting this expression we have the differential equation

$$\frac{d\delta}{da} = \frac{\Omega_m(a)^\gamma}{a} \delta, \quad (2)$$

where γ is the growth index, and $\Omega_m(a) = \Omega_m a^{-3} / E(a)^2$. Here, $E(a) = H(a)/H_0$ is the evolution parameter, $H(a)$ the Hubble parameter, and H_0 its present-day value. It has been shown (see e.g. Linder & Cahn 2007) that for $\gamma \sim 0.55$, Equation 2 accurately reproduces the evolution of δ obtained from Equation 1. Using the Einstein-Boltzmann code CAMB¹ (Lewis et al. 2000), we find that the linear growth $\delta(a)$ obtained from Equation 2 with $\gamma \sim 0.55$ is accurate to better than 0.1 per cent for the relevant scales, redshifts and values of cosmological parameters. Therefore, we adopt $\gamma \sim 0.55$ as a reference, from which to determine departures from GR.

Equation 2 provides a phenomenological model for the growth of density perturbations that allows us to test departures from GR without adopting a particular, fully covariant modified gravity theory. In the absence of such an alternative gravity theory, we perform consistency tests using convenient parameterizations of the background expansion, within GR. We investigate three expansion models that are well tested with current data: flat Λ CDM, a constant dark energy equation of state, w CDM², and non-flat Λ CDM. We can write a general evolution parameter for these models as³

$$E(a) = \left[\Omega_m a^{-3} + \Omega_{\text{de}} a^{-3(1+w)} + \Omega_k a^{-2} \right]^{1/2}, \quad (3)$$

where $w = -1$ for the Λ CDM models, Ω_{de} is the cosmological constant/dark energy density, and Ω_k is the curvature energy density, which is 0 for flat models.

The growth rate $\Omega_m(a)^\gamma$ conveniently tends to 1 in the matter dominated era (high z), thereby matching GR for any value of γ . Thus, we naturally match the initial value of δ in Equation 2 at high- z with that of GR (see Section 3).

3 ANALYSIS OF THE X-RAY LUMINOSITY FUNCTION

We have incorporated the growth index parameterization into the code developed by M08. Briefly, in the XLF analysis, we compare X-ray flux-redshift data from the cluster samples to theoretical predictions. The relation between cluster mass and observed X-ray luminosity is calibrated using deeper pointed X-ray observations (Reiprich & Böhringer 2002).

¹ <http://www.camb.info/>

² This model is only used as an expansion model, and does not assume the presence of dark energy. Therefore, we do not include dark energy density perturbations. The evolution of the density perturbations, due only to matter, are modelled using γ .

³ Although massless neutrinos and photons are included in the analysis, they are negligible at late times.

3.1 Linear theory

The variance of the linearly evolved density field, smoothed by a spherical top-hat window of comoving radius R , enclosing a mass $M = 4\pi\rho_m R^3/3$, is

$$\sigma^2(M, z) = \frac{1}{2\pi^2} \int_0^\infty k^2 P(k, z) |W_M(k)|^2 dk, \quad (4)$$

where $W_M(k)$ is the Fourier transform of the window function, and $P(k, z) \propto k^{n_s} T^2(k, z_t) D(z)^2$ is the linear matter power spectrum as a function of the wavenumber, k , and redshift, z . Here, n_s is the scalar spectral index of the primordial fluctuations, $T(k, z_t)$ is the matter transfer function at redshift z_t , and $D(z) \equiv \delta(z)/\delta(z_t) = \sigma(M, z)/\sigma(M, z_t)$ is the growth factor of linear perturbations, normalized to unity at redshift z_t . We choose $z_t = 30$, well within the matter dominated era (Bertschinger & Zukin 2008). Using CAMB, we calculate $T(k, z_t)$ assuming that GR is valid at early times ($z > z_t$) and that modifications to GR are scale-invariant. For $z < z_t$, we calculate $D(z)$ using Equation 2.

3.2 Non-linear N-body simulations

Using large N-body simulations, Jenkins et al. (2001) and Evrard et al. (2002) showed that the mass function of dark matter halos can be conveniently fitted by the expression

$$f(\sigma^{-1}) \equiv \frac{M}{\rho_m} \frac{dn(M, z)}{d \ln \sigma^{-1}} = A \exp(-|\ln \sigma^{-1} + B|^\epsilon), \quad (5)$$

where $A = 0.316$, $B = 0.67$, and $\epsilon = 3.82$ (Jenkins et al. 2001). These fit values were determined using a spherical overdensity group finder, at 324 times the mean matter density. This formula is approximately ‘universal’ with respect to the cosmology assumed. The universality of this formula has been tested for a wide range of cosmologies (Kuhlen et al. 2005; Lokas et al. 2004; Klypin et al. 2003; Linder & Jenkins 2003; Mainini et al. 2003; Maccio et al. 2004; Francis et al. 2009; Grossi & Springel 2009). Recently Warren et al. (2006) and Tinker et al. (2008) have also reexamined this mass function using a larger suite of simulations.

For linear scales we use the γ -model to test the growth rate for consistency with GR, while for non-linear scales we assume GR⁴. As in M08, we use Equation 5 to predict the number density of galaxy clusters, n , at a given M and z .

⁴ To constrain a particular gravity model, in addition to the expansion history and evolution of the linear density perturbations, we also need the mass function which encompasses the non-linear effects of the model. Recently Schmidt et al. (2009) and Schmidt (2009) have presented halo mass functions for the $f(R)$ and DGP (Dvali et al. 2000) gravity models, respectively. The former work shows that for $f(R)$ models compatible with Solar System tests, equation 5 provides a good fit to the mass function over the relevant mass range within the uncertainties we allow. For more extreme $f(R)$ models, or for less massive clusters (for which non-linear chameleon effects become important) differences arise. For DGP, Schmidt (2009) shows that the mass function for massive halos is significantly suppressed with respect to GR. Such differences can, in principle, be constrained strongly with XLF data.

3.3 Mass–luminosity relation

Following M08, we employ a power-law mass–luminosity relation, assuming self-similar evolution between the mass and X-ray luminosity, L , of massive clusters (e.g. Bryan & Norman 1998). We emphasize, however, that we include a generous allowance for departures from self-similarity, encoded in the parameter ζ ,

$$E(z)M_\Delta = M_0 \left[\frac{L}{E(z)} \right]^\beta (1+z)^\zeta. \quad (6)$$

Here M_Δ is the cluster mass defined at an overdensity of Δ with respect to the critical density, and $\log M_0$ and β are model parameters fitted in the MCMC analysis.

As in M08, we assume a log-normal intrinsic scatter in luminosity for a given mass, η , including this as a model parameter. It is possible that this scatter may evolve with redshift; we, therefore, parameterize the evolution in the scatter as $\eta(z) = \eta_0 (1 + \eta_z z)$, where η_0 is the intrinsic scatter today, and η_z is a parameter that allows for linear evolution in the scatter. Since current data are not able to measure this evolution (see e.g. O’Hara et al. 2006, 2007; Chen et al. 2007), we employ the same conservative prior on η_z used in M08 (see below).

3.4 Priors and systematic allowances

As in M08, our XLF analysis includes five parameters (A , ζ , η_z , B , and s_b)⁵ that are not constrained by current data. We apply the same conservative priors on these parameters as M08.

We apply a Gaussian prior on A , with a mean value of 0.316, and standard deviation of 20 per cent. This deviation conservatively spans the theoretical uncertainty in the mass function of Equation 5. For ζ , we use the uniform prior $(-0.35, 0.35)$, i.e. we allow up to ~ 25 per cent change with respect to self-similar evolution out to $z = 1$. (We also investigate results assuming strictly self-similar evolution, i.e. $\zeta = 0$). For η_z , we use the uniform prior $(-0.3, 0.3)$, i.e., we allow up to ~ 30 per cent evolution in the scatter to $z = 1$.

Departures from hydrostatic equilibrium and sphericity introduce well-known biases in mass measurements from X-ray data. Following M08, we assume a 25 per cent mean bias, and 16 per cent scatter in the bias, with 20 per cent systematic uncertainties in these values, as indicated by hydrodynamical simulations and weak lensing data.

4 INTEGRATED SACHS-WOLFE EFFECT

Through the integrated Sachs-Wolfe (ISW) effect, the low multipoles of the temperature anisotropy power spectrum of the CMB are sensitive to the growth of cosmic structure, and therefore to dark energy and modified gravity models (see e.g. Fang et al. 2008). The ISW effect arises when the gravitational potentials of large scale structures vary with time, yielding a net energetic contribution to the CMB photons crossing them.

⁵ B and s_b are defined in Section 3.1.1 of M08. They parameterize the bias, and the scatter in the bias, expected for hydrostatic mass measurements from X-ray data.

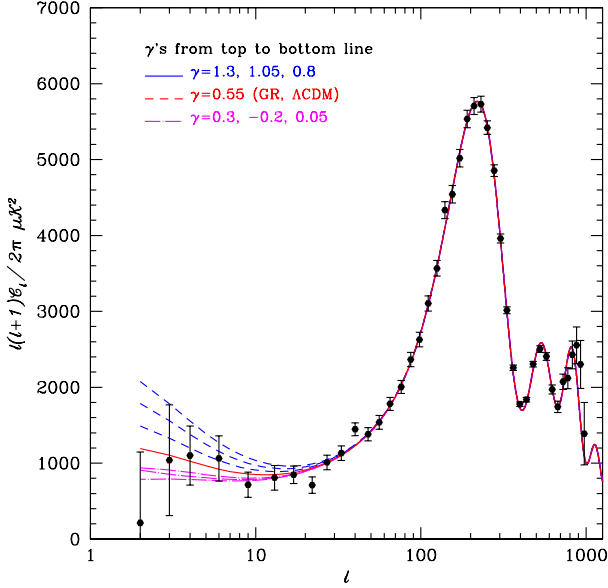


Figure 1. CMB temperature anisotropy power spectra, C_l , for $\gamma = 0.55$ (GR; best-fit Λ CDM model from the five-year WMAP data) (solid, red line), and for values of γ higher than GR (dashed, blue lines), and lower (dot-dashed, magenta lines). The lines are equally spaced in γ . The data are more constraining for the higher values of γ , which produce larger changes in the ISW effect and significantly worse fits to the data. Higher values of γ monotonically increase the ISW effect while lower values first decrease it and then increase it (see a similar behaviour in Hu 2008). The circles are the binned WMAP5 data.

On large scales, we calculate the transfer function due to the ISW effect as (Weller & Lewis 2003)

$$\Delta_l^{\text{ISW}}(k) = 2 \int dt e^{-\tau(t)} \phi' j_l [k(t - t_0)] \quad (7)$$

where ‘prime’ denotes a derivative with respect to the conformal time t , t_0 is the conformal time today, τ is the optical depth to the last scattering, and $j_l(x)$ is the spherical Bessel function for the multipole l . The total transfer function is the sum of Equation 7 and the transfer function from the last scattering surface (LSS), $\Delta_l(k) = \Delta_l^{\text{ISW}}(k) + \Delta_l^{\text{LSS}}(k)$. From this, we calculate the anisotropy power spectrum of the temperature fluctuations C_l (see Figure 1).

For GR, we can calculate the gravitational potential ϕ using the Poisson equation $k^2 \phi = -4\pi G a^2 \delta\rho_m$, for which ϕ depends only on the matter density perturbations $\delta\rho_m$ ⁶. Here we use the γ -model to test CMB data for consistency with GR, restricting ourselves to departures from GR in which the ISW effect can be calculated, as in GR, using the Poisson equation at all scales⁷.

⁶ Using CAMB we have verified this for the relevant region of parameter space. The other two components of the Weyl tensor that would contribute to ϕ , the anisotropic stress and energy flux (for details on these terms see Challinor & Lasenby 1999), are negligible.

⁷ For a general gravity model, none of the components of the Weyl tensor will be negligible and, therefore modifications to the

The ISW effect is only relevant at $z < 2$. For this redshift range, we modify CAMB to calculate the evolution of δ , and therefore ϕ' , using Equation 2, and obtain

$$\phi' = 4\pi G \frac{a^2}{k^2} \dot{a} \delta\rho_m [1 - \Omega_m(a)^\gamma]. \quad (8)$$

We calculate $\Delta_l^{\text{ISW}}(k)$ at $z = 2$ using GR, and use these values as initial conditions when evolving to $z = 0$ in the γ -model.

5 DATA ANALYSIS

We use the five-year WMAP CMB data (Dunkley et al. 2009; Komatsu et al. 2009, and references therein), SNIa data from the ‘‘Union’’ compilation of Kowalski et al. (2008), the f_{gas} measurements of Allen et al. (2008), and XLF data from the BCS ($z < 0.3$, northern sky; Ebeling et al. 1998), REFLEX ($z < 0.3$, southern sky; Böhringer et al. 2004), MACS ($0.3 < z < 0.7$, ~ 55 per cent sky coverage; Ebeling et al. 2001, 2007), and 400sd ($z < 0.9$, ~ 1 per cent sky coverage; Burenin et al. 2007) cluster samples. Adopting a luminosity limit of $2.55 \times 10^{44} h_{70}^{-2} \text{erg s}^{-1}$ ($0.1 - 2.4 \text{keV}$), we use 78 clusters above a flux limit of $4.4 \times 10^{-12} \text{erg s}^{-1} \text{cm}^{-2}$ from BCS, 130 above $3.0 \times 10^{-12} \text{erg s}^{-1} \text{cm}^{-2}$ from REFLEX, 34 above $2 \times 10^{-12} \text{erg s}^{-1} \text{cm}^{-2}$ from MACS, and 30 above $0.14 \times 10^{-12} \text{erg s}^{-1} \text{cm}^{-2}$ from the 400sd survey.

We use a Metropolis MCMC algorithm to calculate the posterior probability distributions of our model parameters. We use a modified version of the COSMOMC⁸ code (Lewis & Bridle 2002) that includes additional modules to calculate the likelihood for the f_{gas} experiment⁹ (Allen et al. 2008), and for the XLF experiment (M08).

When we use flat Λ CDM as background model we fit seven cosmological parameters: the mean physical baryon density, $\Omega_b h^2$; the mean physical dark matter density, $\Omega_c h^2$; the (approximate) ratio of the sound horizon at last scattering to the angular diameter distance, θ (which is less correlated with other parameters than H_0 , as shown by Kosowsky et al. 2002); the optical depth to reionization, τ ; the adiabatic scalar spectral index, n_s ; the logarithm of the adiabatic scalar amplitude, $\ln(A_s)$; and the growth index, γ . For the flat w CDM background model, we have w as an additional parameter; and for the non-flat Λ CDM model, Ω_k . We marginalize over seven other parameters that model systematic uncertainties in the f_{gas} analysis (see details in Allen et al. 2008), and seven more that account for uncertainties in the XLF analysis. For the SNIa analysis, we use, as provided by Kowalski et al. (2008), a covariance matrix that accounts for systematic uncertainties.

Poisson equation will be required (see e.g. Hu & Sawicki 2007; Hu 2008). Interestingly, for the DGP gravity model, Sawicki et al. (2007) showed that the used of an appropriately modified Poisson equation near the horizon yields an enhancement of the ISW effect, and thus stronger constraints with CMB data.

⁸ <http://cosmologist.info/cosmomc/>

⁹ http://www.stanford.edu/~drapetti/fgas_module/

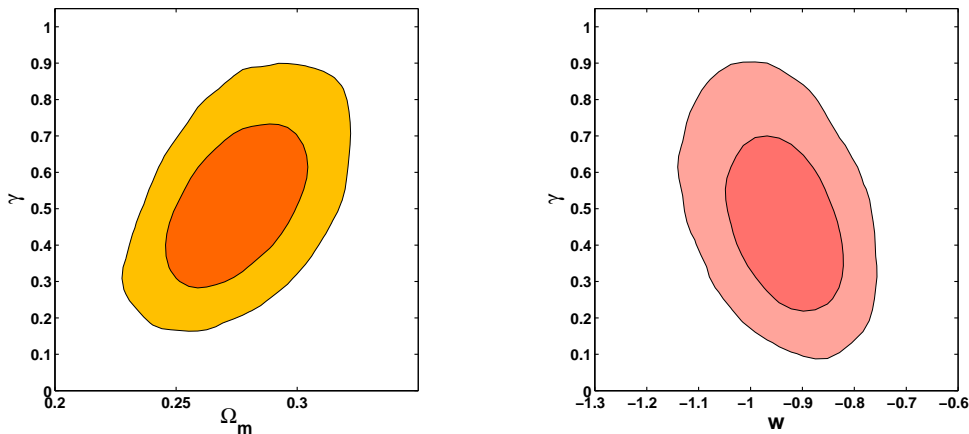


Figure 2. 68 and 95 per cent confidence contours in the (left panel) Ω_m, γ plane for the flat Λ CDM background model, and (right panel) w, γ plane for the flat w CDM model, from the combination of XLF, CMB, SNIa, and f_{gas} data. These results do not include the (subdominant) contribution from the ISW effect (see text and Table 1 for details).

6 RESULTS

As shown in Allen et al. (2008) and references therein, the combination of f_{gas} , SNIa, and CMB data places tight constraints on the expansion history and Ω_m . The addition of the XLF data allows us to place tight constraints on γ . Assuming a flat Λ CDM background model, we obtain the results shown in the left panel of Figure 2. The results for a flat, constant- w model are shown in the right panel of Figure 2. The marginalized values are summarized in Table 1. For flat Λ CDM we find $\gamma = 0.51^{+0.16}_{-0.15}$. Interestingly, when allowing w to be free, we obtain similar constraints of $\gamma = 0.44^{+0.17}_{-0.15}$. We also see an anticorrelation between γ and w , wherein models close to a cosmological constant ($w = -1$) are most consistent with GR ($\gamma \sim 0.55$). We have also investigated the effect of relaxing the assumption of flatness in the Λ CDM model and find $\gamma = 0.51^{+0.19}_{-0.16}$, with no significant covariance between γ and Ω_k .

For massive clusters, such as those in the current XLF data set, self-similar evolution of the mass-luminosity relation is a well-motivated theoretical prediction (Bryan & Norman 1998). Current Chandra data (Mantz et al., submitted) show good agreement with this prediction over the redshift range spanned by the XLF data ($z < 0.5$). Under the assumption of strictly self-similar evolution ($\zeta = 0$), we find $\gamma = 0.44^{+0.12}_{-0.11}$ for the flat Λ CDM background model.

As discussed in Section 4, the low multipoles of the CMB are also sensitive to the growth rate through the ISW effect. Even though the ISW data currently have less constraining power on γ than the XLF¹⁰, adding the ISW leads to ~ 17 per cent tighter constraints on γ : for the flat Λ CDM background model we obtain $\gamma = 0.45^{+0.14}_{-0.12}$, for flat w CDM $\gamma = 0.42^{+0.14}_{-0.13}$, and $\gamma = 0.50^{+0.16}_{-0.15}$ for non-flat Λ CDM.

Table 1. Marginalized 1σ constraints on Ω_m , σ_8 , and γ , using all the data sets without (default) or with (default+ISW) the ISW effect, for the flat Λ CDM (A), flat w CDM (B), and non-flat Λ CDM (C) expansion history models. For the B model we obtain $w = -0.93 \pm 0.07$. The results for Ω_m are the same with or without the ISW.

	$\Omega_m, \sigma_8, \gamma$ (default)			σ_8, γ (default+ISW)	
A	$0.27^{+0.02}_{-0.02}$	$0.82^{+0.05}_{-0.04}$	$0.51^{+0.16}_{-0.15}$	$0.83^{+0.04}_{-0.04}$	$0.45^{+0.14}_{-0.12}$
B	$0.28^{+0.02}_{-0.02}$	$0.81^{+0.05}_{-0.05}$	$0.44^{+0.17}_{-0.15}$	$0.82^{+0.04}_{-0.04}$	$0.42^{+0.14}_{-0.13}$
C	$0.31^{+0.04}_{-0.03}$	$0.76^{+0.06}_{-0.04}$	$0.51^{+0.19}_{-0.16}$	$0.77^{+0.05}_{-0.05}$	$0.50^{+0.16}_{-0.15}$

7 CONCLUSIONS

Combining XLF, f_{gas} , SNIa and CMB data, we have simultaneously constrained the background evolution of the Universe and the growth of matter density fluctuations on cosmological scales, allowing us to search for departures from GR. We parameterize the expansion history with simple models that include late-time cosmic acceleration, taking flat Λ CDM as our default model, but also investigating flat, constant w models, and non-flat Λ CDM models. We parameterize the growth of cosmic structure using the growth index, γ , which assumes the same scale dependence as GR, but allows for time-dependent deviations from it.

We have performed MCMC analyses with seven (or eight) interesting cosmological parameters, and an additional fourteen parameters to encompass conservative allowances for systematic uncertainties. Marginalizing over these allowances, we obtain the tightest constraints to date on the growth index. For the flat Λ CDM background model, we measure $\gamma = 0.51^{+0.16}_{-0.15}$. Allowing w or Ω_k to be free, we obtain similar constraints: $\gamma = 0.44^{+0.17}_{-0.15}$ and $\gamma = 0.51^{+0.19}_{-0.16}$, respectively. Including also constraints on γ from the ISW effect, we obtain $\gamma = 0.45^{+0.14}_{-0.12}$ for flat Λ CDM. Currently, we find no evidence for departures from General Relativity.

In the near future, improved XLF analyses should provide significantly tighter constraints on both γ and ζ , allowing us to explore more complex modified gravity models (Rapetti et al., in preparation). Our results highlight the

¹⁰ Note that the cross-correlation of the ISW effect with galaxy surveys (see e.g. Ho et al. 2008; Lombriser et al. 2009) may provide competitive, additional constraint on γ .

importance of X-ray cluster data, and the potential of combined expansion history plus growth of structure studies, for testing dark energy and modified gravity models for the acceleration of the Universe.

ACKNOWLEDGMENTS

We thank A. Lewis, M. Amin, R. Blandford, P. Wang, W. Hu, L. Lombriser and I. Sawicki for useful discussions. We thank G. Morris for technical support. The computational analysis was carried out using the KIPAC XOC and Orange computer clusters at SLAC. We acknowledge support from the National Aeronautics and Space Administration through Chandra Award Numbers DD5-6031X and G08-9118X issued by the Chandra X-ray Observatory Center, which is operated by the Smithsonian Astrophysical Observatory for and on behalf of the National Aeronautics and Space Administration under contract NAS8-03060. This work was supported in part by the U.S. Department of Energy under contract number DE-AC02-76SF00515.

REFERENCES

- Acquaviva V., Hajian A., Spergel D. N., Das S., 2008, *Phys. Rev.*, D78, 043514
- Allen S. W., Rapetti D. A., Schmidt R. W., Ebeling H., Morris R. G., Fabian A. C., 2008, *MNRAS*, 383, 879
- Allen S. W., Schmidt R. W., Ebeling H., Fabian A. C., van Speybroeck L., 2004, *MNRAS*, 353, 457
- Amin M. A., Wagoner R. V., Blandford R. D., 2008, *MNRAS*, 390, 131
- Ballesteros G., Riotto A., 2008, *Phys. Lett.*, B668, 171
- Bertschinger E., Zukin P., 2008, *Phys. Rev.D*, 78, 024015
- Böhringer H., et al., 2004, *Astron. Astrophys.*, 425, 367
- Bryan G. L., Norman M. L., 1998, *Astrophys. J.*, 495, 80
- Burenin R. A., Vikhlinin A., Hornstrup A., Ebeling H., Quintana H., Mescheryakov A., 2007, *ApJ S.*, 172, 561
- Caldwell R., Cooray A., Melchiorri A., 2007, *Phys. Rev.*, D76, 023507
- Carroll S. M., Sawicki I., Silvestri A., Trodden M., 2006, *New J. Phys.*, 8, 323
- Challinor A., Lasenby A., 1999, *Astrophys. J.*, 513, 1
- Chen Y., Reiprich T. H., Böhringer H., Ikebe Y., Zhang Y.-Y., 2007, *Astron. Astrophys.*, 466, 805
- Cole S., et al., 2005, *MNRAS*, 362, 505
- Davis T. M., et al., 2007, *Astrophys. J.*, 666, 716
- Di Porto C., Amendola L., 2008, *Phys. Rev.*, D77, 083508
- Dore O., et al., 2007, *arXiv:0712.1599*
- Dunkley J., et al., 2009, *ApJ S.*, 180, 306
- Dvali G. R., Gabadadze G., Porrati M., 2000, *Phys. Lett.*, B485, 208
- Ebeling H., Barrett E., Donovan D., Ma C.-J., Edge A. C., van Speybroeck L., 2007, *ApJ Lett.*, 661, L33
- Ebeling H., Edge A. C., Henry J. P., 2001, *ApJ*, 553, 668
- Ebeling H., et al., 1998, *MNRAS*, 301, 881
- Eisenstein D. J., et al., 2005, *ApJ*, 633, 560
- Evrard A. E., et al., 2002, *ApJ*, 573, 7
- Fang W., Wang S., Hu W., Haiman Z., Hui L., May M., 2008, *Phys. Rev.D*, 78, 103509
- Francis M. J., Lewis G. F., Linder E. V., 2009, *MNRAS*, 394, 605
- Frieman J. A., Turner M. S., Huterer D., 2008, *ARA&A*, 46, 385
- Gannouji R., Polarski D., 2008, *JCAP*, 0805, 018
- Gong Y., 2008, *Phys. Rev.D*, 78, 123010
- Grossi M., Springel V., 2009, *MNRAS*, 394, 1559
- Ho S., Hirata C., Padmanabhan N., Seljak U., Bahcall N., 2008, *Phys. Rev.D*, 78, 043519
- Hu W., 2008, *Phys. Rev.*, D77, 103524
- Hu W., Sawicki I., 2007, *Phys. Rev.*, D76, 104043
- Huterer D., Linder E. V., 2007, *Phys. Rev.*, D75, 023519
- Jenkins A., Frenk C. S., White S. D. M., Colberg J. M., Cole S., Evrard A. E., Couchman H. M. P., Yoshida N., 2001, *MNRAS*, 321, 372
- Klypin A., Maccio A. V., Mainini R., Bonometto S. A., 2003, *Astrophys. J.*, 599, 31
- Komatsu E., et al., 2009, *ApJ S.*, 180, 330
- Kosowsky A., Milosavljevic M., Jimenez R., 2002, *Phys. Rev.*, D66, 063007
- Kowalski M., et al., 2008, *ApJ*, 686, 749
- Kuhlen M., Strigari L. E., Zentner A. R., Bullock J. S., Primack J. R., 2005, *MNRAS*, 357, 387
- Lahav O., Lilje P. B., Primack J. R., Rees M. J., 1991, *MNRAS*, 251, 128
- Lewis A., Bridle S., 2002, *Phys. Rev.D*, 66, 103511
- Lewis A., Challinor A., Lasenby A., 2000, *Astrophys. J.*, 538, 473
- Linder E. V., 2005, *Phys. Rev.*, D72, 043529
- Linder E. V., Cahn R. N., 2007, *Astropart. Phys.*, 28, 481
- Linder E. V., Jenkins A., 2003, *MNRAS*, 346, 573
- Lokas E. L., Bode P., Hoffman Y., 2004, *MNRAS*, 349, 595
- Lombriser L., Hu W., Fang W., Seljak U., 2009, *arXiv:0905.1112*
- Maccio A. V., Quercellini C., Mainini R., Amendola L., Bonometto S. A., 2004, *Phys. Rev.*, D69, 123516
- Mainini R., Maccio A. V., Bonometto S. A., 2003, *New Astron.*, 8, 173
- Mantz A., Allen S. W., Ebeling H., Rapetti D., 2008, *MNRAS*, 387, 1179, (M08)
- Mortonson M. J., Hu W., Huterer D., 2009, *Phys. Rev.D*, 79, 023004
- Nesseris S., Perivolaropoulos L., 2008, *Phys. Rev.*, D77, 023504
- O'Hara T. B., Mohr J. J., Bialek J. J., Evrard A. E., 2006, *ApJ*, 639, 64
- O'Hara T. B., Mohr J. J., Sanderson A. J. R., 2007, *arXiv:0710.5782*
- Peebles P. J. E., 1980, *The large-scale structure of the universe*. Princeton University Press, 1980.
- Percival W. J., Cole S., Eisenstein D. J., Nichol R. C., Peacock J. A., Pope A. C., Szalay A. S., 2007, *MNRAS*, 381, 1053
- Perlmutter S., et al., 1999, *ApJ*, 517, 565
- Polarski D., Gannouji R., 2008, *Phys. Lett.*, B660, 439
- Rapetti D., Allen S. W., Amin M. A., Blandford R. D., 2007, *MNRAS*, 375, 1510
- Rapetti D., Allen S. W., Weller J., 2005, *MNRAS*, 360, 555
- Reiprich T. H., Böhringer H., 2002, *ApJ*, 567, 716
- Riess A. G., et al., 1998, *ApJ*, 116, 1009
- Sapone D., Amendola L., 2007, *arXiv:0709.2792*

- Sawicki I., Song Y.-S., Hu W., 2007, *Phys. Rev.*, D75, 064002
Schmidt F., 2009, *Phys. Rev.D*, 80, 043001
Schmidt F., Lima M., Oyaizu H., Hu W., 2009, *Phys. Rev.D*, 79, 083518
Spergel D. N., et al., 2003, *ApJ S.*, 148, 175
Spergel D. N., et al., 2007, *Astrophys. J. Suppl.*, 170, 377
Thomas S. A., Abdalla F. B., Weller J., 2009, *MNRAS*, 395, 197
Tinker J., et al., 2008, *ApJ*, 688, 709
Vikhlinin A., et al., 2009, *Astrophys. J.*, 692, 1060
Wang L.-M., Steinhardt P. J., 1998, *Astrophys. J.*, 508, 483
Warren M. S., Abazajian K., Holz D. E., Teodoro L., 2006, *Astrophys. J.*, 646, 881
Wei H., 2008, *Phys. Lett.*, B664, 1
Weller J., Lewis A. M., 2003, *MNRAS*, 346, 987